Bull. Mater. Sci., Vol. 38, No. 5, September 2015, pp. 1359–1365. © Indian Academy of Sciences.

Red luminescence from ZnO : Cr^{3+} nanophosphors under visible excitation

N PUSHPA[1], M K KOKILA[1,*], B M NAGABHUSHANA[2], H NAGABHUSHANA[3] and A JAGANNATHA REDDY[4]

[1]Department of Physics, Bangalore University, Bangalore 560 056, India
[2]Department of Chemistry, M.S. Ramaiah Institute of Technology, Bangalore 560 054, India
[3]Prof. C.N.R. Rao Centre for Advanced Materials Research, Tumkur University, Tumkur 572 103, India
[4]Department of Physics, M.S. Ramaiah Institute of Technology, Bangalore 560 054, India

MS received 27 March 2014; accepted 20 April 2015

Abstract. **ZnO : Cr^{3+} (1 mol%) nanophosphor is synthesized by the wet chemical solution combustion method at the temperature of 400°C. Powder X-ray diffraction results confirmed that Cr^{3+}-doped and undoped ZnO nanophosphors exhibit hexagonal wurtzite structure. The average crystallite size calculated from Scherrer's method is 25 nm for undoped and 14 nm for Cr^{3+}-doped ZnO. The UV–visible absorption spectra shows red shift in Cr^{3+}-doped ZnO. Photoluminescence studies of undoped ZnO show violet emission peak at 400 nm and blue emission peak at 447 nm. Cr^{3+}-doped ZnO shows red emission peaks at 642, 694 and 746 nm, which are mainly attributed to spin forbidden transitions of $^2E_g \rightarrow {}^4A_{2g}$ of Cr^{3+} ion in ZnO : Cr^{3+} nanophosphor. Thermoluminescence (TL) studies recorded at a heating rate of 6°C s^{-1} show two well-resolved glow peaks at 124 and 284°C. It is found that the TL intensity increases with the gamma irradiation dose (500 Gy–10 kGy).**

Keywords. **Solution combustion synthesis; PXRD; SEM; photoluminescence; thermoluminescence; UV–visible spectroscopy.**

1. Introduction

ZnO is considered to be one of the most important oxide materials, owing to its unique features and wide range of technological applications. ZnO is a II–VI semiconductor with wide bandgap (3.37 eV) and large exciton binding energy (60 meV). It is a very good promising material for many applications such as UV absorption, spintronics, photocatalysis, sensing and UV light-emitting devices. But these properties of ZnO strongly depend on the impurities and defects.[1–3] It is well known that the existence of defects in a semiconductor would lead to corresponding defects energy levels in the bandgap.[4] Therefore, it was believed and reported by many researchers that the different transition metal dopants such as (Ni, Cr, Mn, Cu, Co, etc.) help in altering the properties of ZnO.[5–11] In recent times, several research groups prepared the chromium-doped ZnO nanoparticles and reported that there is only a pronounced near-band edge emission (NBE) upon chromium doping, but there is no origin of any new photoluminescence (PL) emission.[12–14] But reported studies on chromium doped other nanomaterials shows red emission.[15,16] These controversial consequences indicated that luminescence property of Cr-doped ZnO is very sensitive with respect to shape, size (bulk, nanoparticle, thin film), preparation conditions and doping concentrations and are still debatable, thus research work in this field is still in its infancy. A number of methods have been developed for the synthesis of the ZnO nanoparticles, such as the hydrothermal,[17] sol–gel,[18] co-precipitation,[6] solution combustion method[19] and so on. Among these methods solution combustion technique is of great interest because of its simplicity, low cost and effective low temperature factors, which can give rise to better quality nanoparticles of desired size and shape.

Although there are several reports on chromium-doped ZnO[12–14] and other nanoparticles,[16,20] the luminescence study of chromium-doped ZnO nanomaterials is very rare. In light of this, present work reports on luminescence studies of undoped and 1 mol% Cr^{3+}-doped ZnO nanophosphors prepared by the solution combustion method. The synthesized samples are well characterized using powder X-ray diffraction (PXRD), scanning electron microscopy (SEM), Fourier-transform infrared (FTIR) and UV–visible spectroscopic techniques and their PL and thermoluminescence (TL) are discussed in detail.

*Author for correspondence (drmkkokila@gmail.com)

2. Experimental

2.1 *Synthesis*

Undoped and 1 mol% Cr^{3+}-doped ZnO powders are synthesized via the low-temperature solution combustion method. The stoichiometric quantities of analytical grade $Zn(NO_3)_2$, $Cr(NO_3)_3$ and fuel $C_{12}H_{22}O_{11}$ are dissolved in a minimum quantity of double distilled water, keeping total oxidizing (O) and reducing (F) valencies of the components equal to unity (i.e., O/F = 1). The Petri dish containing this solution is placed in a preheated muffle furnace set at 400°C. The mixture underwent dehydration at lower temperatures and decomposition, resulting in the simultaneous evolution of large amounts of gases. This exothermic reaction resulted in the voluminous and fluffy product. The whole process lasted for about 10 min. The dish is then taken out of the furnace and the product is crushed into a fine powder. The as-formed powder is calcined at 500°C for 10 min and characterization is done.

3. Results and discussion

3.1 *PXRD*

Figure 1 illustrates the PXRD pattern of the undoped and Cr^{3+}-doped ZnO nanopowders. The sharp diffraction peaks manifest that ZnO nanoparticles have high crystallinity. All the PXRD peaks are well matched with the standard hexagonal wurtzite structure of ZnO (JCPDS card no. 36-1451). No other peaks related to any secondary or impurity phases are detected, which confirms the phase purity of the sample. A small shift in the position of the main peak (inset of figure 1) to the lower side of 2θ values and broadening of PXRD peaks are observed in the Cr^{3+}-doped sample, due to smaller ionic radius of Cr^{3+} (0.063 nm) than that of Zn^{2+} (0.074 nm). This observation is similar in the case of transition metal-doped ZnO (Fe, Cu, Ni).[21]

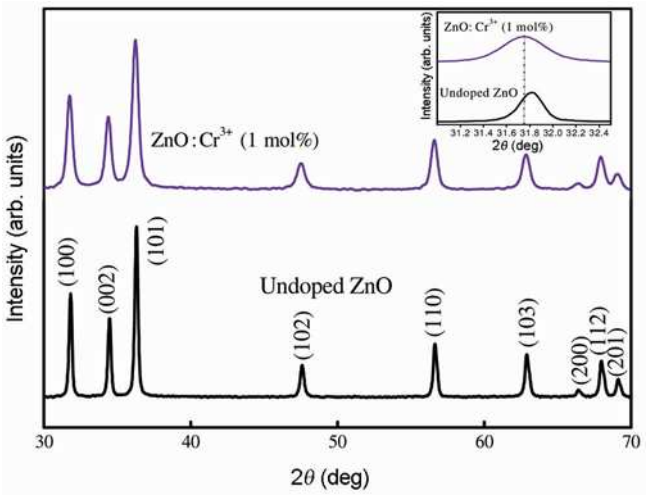

Figure 1. PXRD of undoped and Cr^{3+}-doped ZnO.

The average crystallite size of the particles (D) for each reflection is estimated by Scherrer's formula.[22] The average crystallite size of Cr^{3+}-doped sample (14 nm) is found to be less when compared to undoped ZnO (25 nm).

3.2 *SEM*

The morphology of the combustion-derived products are characterized by SEM. Figure 2 shows SEM images of undoped ZnO nanopowders (figure 2a and b) and Cr^{3+}-doped ZnO powders (figure 2c and d). It is observed that undoped ZnO nanopowders are less porous in nature (figure 2b) compared to Cr^{3+}-doped nanopowders (figure 2d). During the combustion process, several gases are evolved and hence the combustion products are porous with voids as shown in the micrographs.

3.3 *FTIR*

The molecular structure and purity of prepared nanopowders are analysed by FTIR spectroscopy. Figure 3 shows the FTIR spectra of undoped and Cr^{3+}-doped nanophosphors, which are acquired in the range of 400–4000 cm^{-1}. The peak at 3428 cm^{-1} corresponding to O–H stretching vibration is due to small trace of water, existing in prepared ZnO nanopowders. The peak at 420 cm^{-1} is ascribed to Zn–O stretching vibration. No other impurity peaks related to any other groups show the purity of the prepared nanopowder.

3.4 *UV–visible absorption spectra*

The UV absorbance spectra of undoped and Cr^{3+}-doped ZnO nanopowders are shown in figure 4. The strong absorption peak at 375 nm for undoped ZnO is the characteristic band of the wurtzite hexagonal ZnO. A red shift in the absorption peak is observed in Cr^{3+}-doped ZnO, which may be related to the formation of shallow levels inside the bandgap due to doping.

The bandgap E_g is calculated using Tauc relation[22]

$$\alpha h\nu \approx (h\nu - E_g)^{1/2}, \quad (1)$$

where $h\nu$ is the photon energy and α the optical absorption coefficient near the fundamental absorption edge. The optical bandgap (E_g) is obtained by plotting $(\alpha h\nu)^2$ *vs.* $h\nu$ in the high absorption range followed by extrapolating the linear region of the plots $(\alpha h\nu)^2 = 0$ (figure 5).

It is evident that Cr^{3+}-doped ZnO has bandgap of 3.05 eV when compared to undoped ZnO (3.3 eV). The

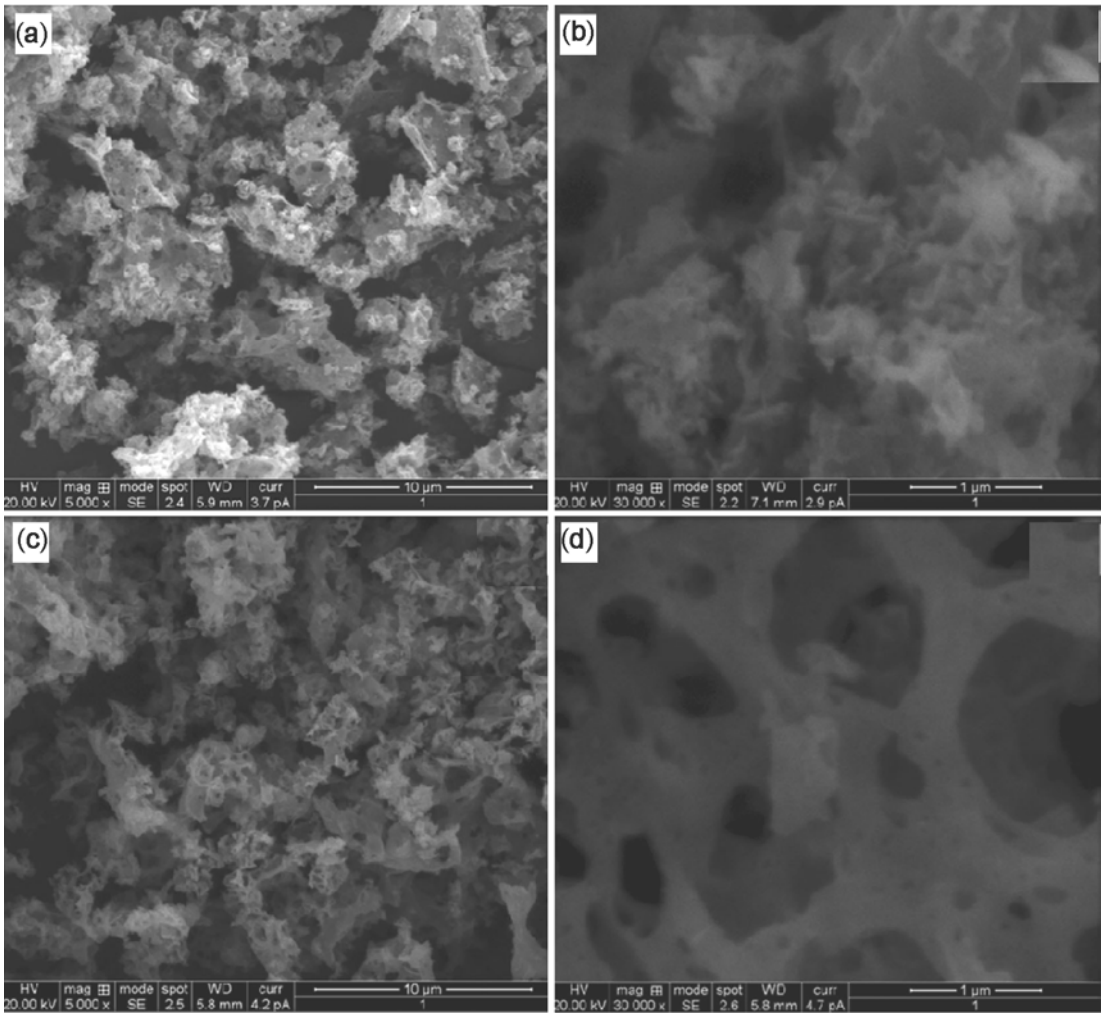

Figure 2. SEM images of (**a** and **b**) undoped and (**c** and **d**) 1 mol% Cr^{3+}-doped ZnO nanopowders.

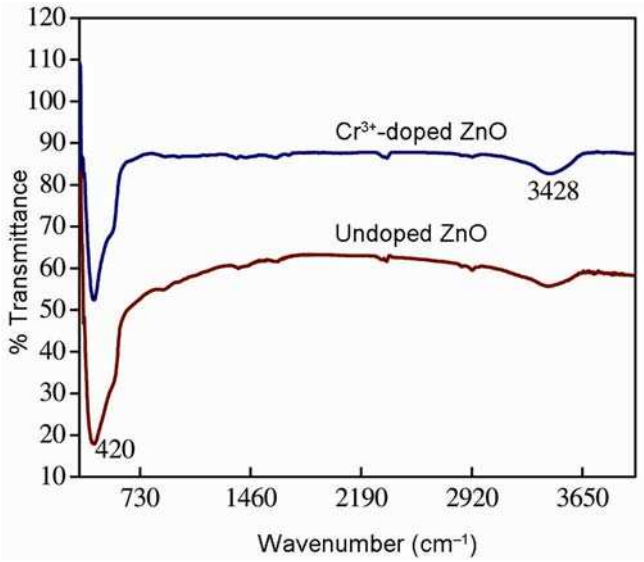

Figure 3. FTIR spectra of undoped and Cr^{3+}-doped ZnO.

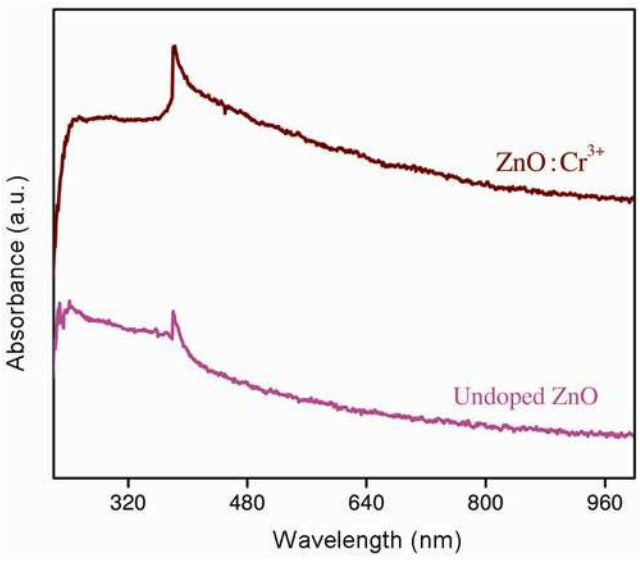

Figure 4. UV–visible absorption spectrum of undoped and Cr^{3+}-doped ZnO.

decrease in E_g with Cr^{3+} doping is attributed to the s–d and p interactions and smaller average grain size.[23]

3.5 *PL studies*

The PL emission and excitation spectra recorded for undoped ZnO is shown in figure 6. The excitation spectrum monitored for 400 nm gives a very broad peak at 325 nm. The emission spectrum is recorded under 325 nm excitation, shows the more intense UV emission peak at 400 nm and corresponds to NBE emission of the wide bandgap ZnO due to the exciton transition from the localized level below the conduction band to the valence band.[24] The less intense broad emission band at 447 nm in the visible region indicates the transition from Zinc interstitial (Zn_i) to the impurity level.[25,26] The blue-green emission at 484 nm is due to radiative transition of an electron from the deep donor level of Zn_i to an acceptor level of neutral V_{Zn}; green emission peak 524 nm corresponds to the electron transition from the bottom of the conduction band to the antisite defect O_{Zn} level, as illustrated in the energy level diagram (figure 8) representing the emission probabilities from respective luminescence centres.[27,28] Lin and co-workers[29] reported the PL emission peaks of ZnO thin films based on defects energy level.

The PL (emission and excitation) spectra of Cr^{3+}-doped ZnO at room temperature is shown in figure 7. Under excitation at 462 nm, the material exhibits a sharp red emission peak at 693 nm mainly due to spin forbidden transition of $^2E \rightarrow {}^4A_2$ of Cr^{3+} ions, less intense peaks at

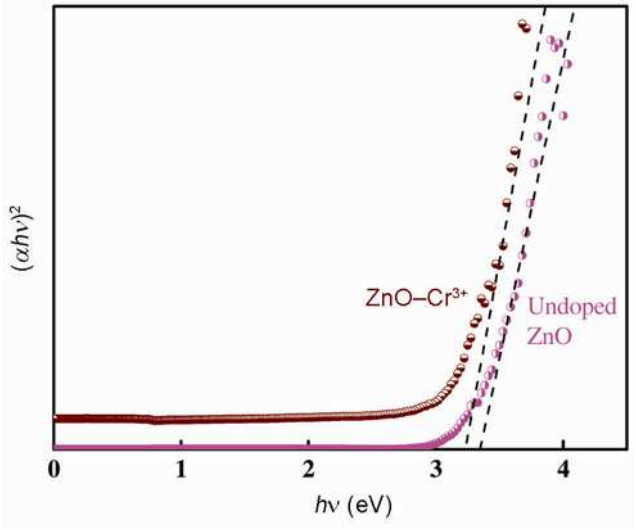

Figure 5. Bandgap of undoped and Cr^{3+}-doped ZnO nanopowders.

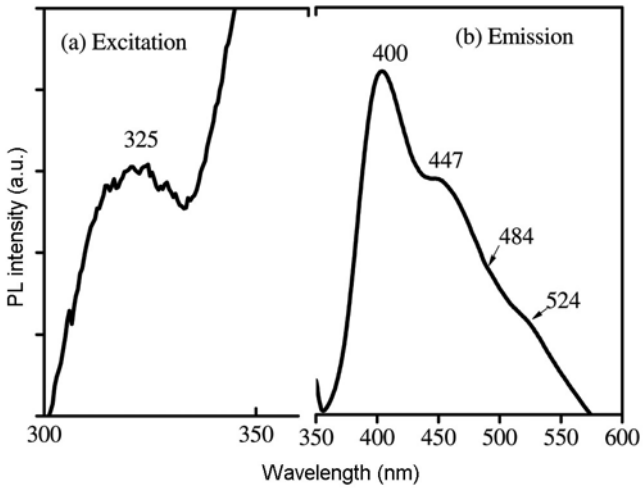

Figure 6. Photoluminescence spectrum of undoped ZnO nanophosphor.

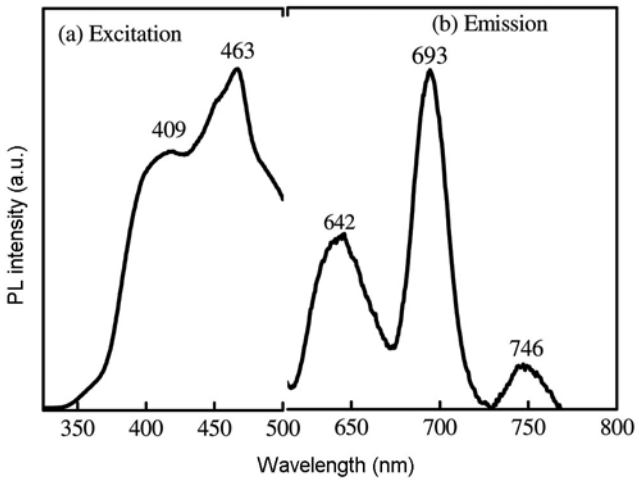

Figure 7. Photoluminescence spectrum of 1 mol% Cr^{3+}-doped ZnO.

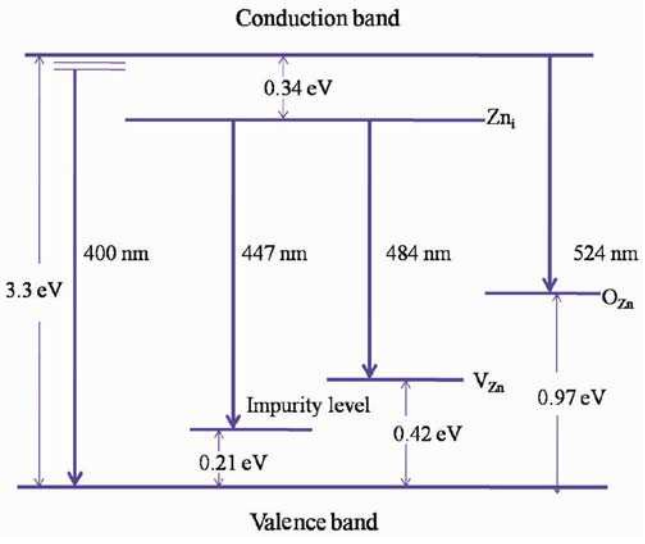

Figure 8. Defects present in the bandgap of ZnO.

642 and 746 nm may be due to the phonon side bands[16] of $^2E \rightarrow {}^4A_2$. The excitation spectrum monitored for 693 nm covers a very broad spectral region (from 350 to 500 nm) and consists of two main excitation peaks at 409 and 463 nm which are originating from $^4A_2 \rightarrow {}^4T_1$ (^4F) transitions [30] as shown in figure 9.

The CIE colour co-ordinates measured from PL emission of undoped and Cr^{3+}-doped nanoparticles are shown in figure 10. The CIE *x* and *y* values for undoped ZnO are 0.18 and 0.19, respectively (point (b)) and confirm 'BLUE' emission, whereas CIE *x* and *y* values for Cr^{3+}-doped ZnO nanoparticles are 0.54 and 0.46, respectively (point (a)), confirm near 'RED' emission.

3.6 *TL*

Figure 11 shows the TL glow curves of ZnO : Cr^{3+} nanoparticles irradiated with gamma rays of dose ranges from 500 Gy to 10 kGy, measured at a heating rate of 6°C s^{-1}. Two well-resolved TL glow peaks at 124 and 284°C with the enhancement in TL intensity, due to high concentration of luminescence centres caused by increasing the radiation, is observed. There is no appreciable shift in the glow peak position with the increase in gamma dose. The appearance of two peaks in the glow curve indicates that there are possibly two kinds of trapping sites generated due to gamma irradiation, which are mainly shallow and deeper traps, respectively, at 124 and 284°C. It is observed from figure 12 that for 6–8 kGy gamma dosage the deeper traps (284°C) show more intense glow peak. Hence, overlapping of peaks as shown in figure 11 is observed. Recently, Cruz-Vazquez and co-workers[31] reported the thermostimulated luminescence of microcrystalline

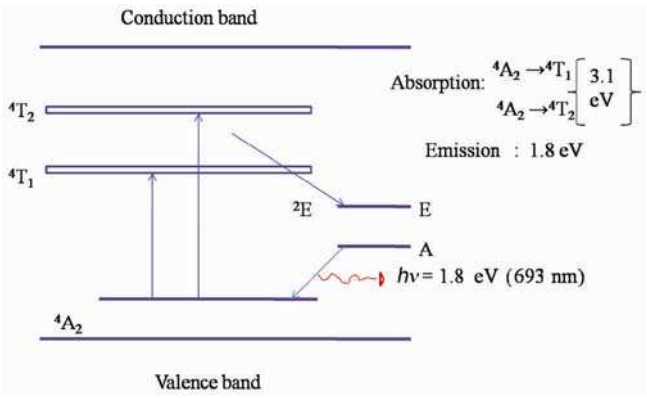

Figure 9. Schematic representation of transitions in Cr^{3+} ions.

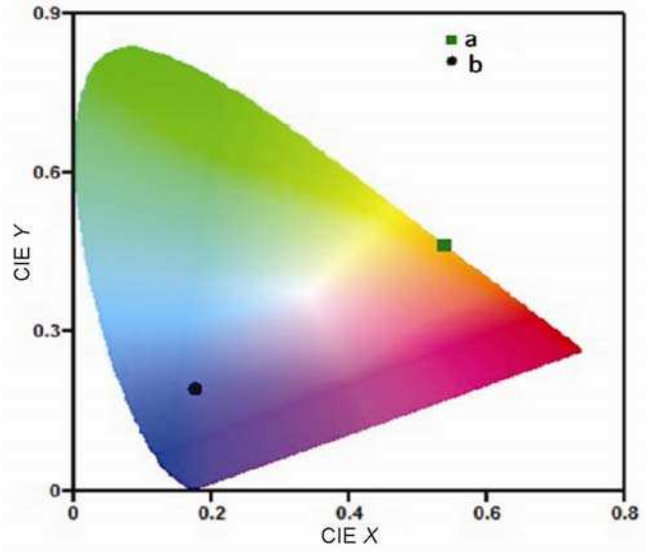

Figure 10. CIE chromaticity diagram of undoped and Cr^{3+} doped ZnO.

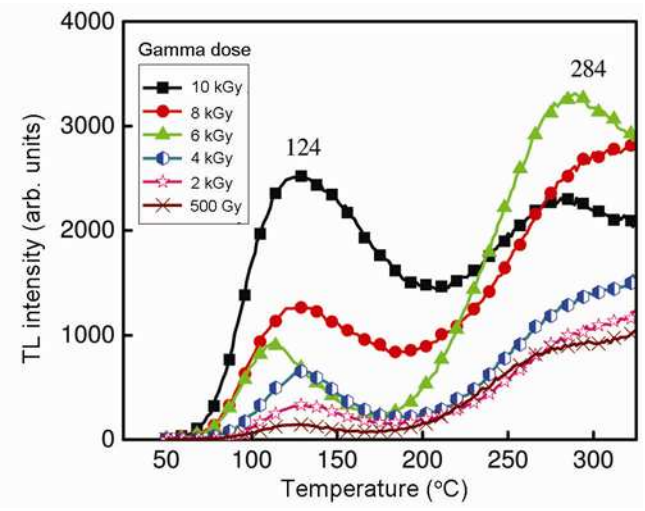

Figure 11. TL glow curves of ZnO : Cr^{3+} nanopowders irradiated with γ-rays.

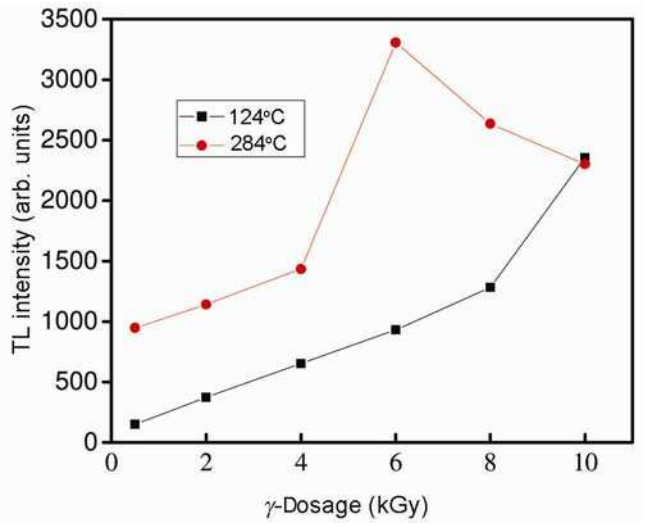

Figure 12. Variation of TL intensity with γ-dosage.

$ZnO–CdSO_4$ composites exposed to beta irradiation (50–300 Gy), which exhibits two glow peaks at 112 and 216°C and overlapping of peaks was observed. The similar overlapping was observed for the ZnO nanoneedles.[32]

TL glow curve analysis helps in the estimation of localized trap depth and frequency factor (s), which gives information about the electrons that are released from the trap due to thermal energy. They may get retrapped at the trapping centre, which is known as second-order kinetics. On the other hand, the thermally released electrons may reach the conduction band without getting retrapped and it is known as first-order kinetics. Further, it has been observed that the glow curves are more symmetric in nature on a wide temperature scale. This is one of the characteristic features of a second-order TL glow curve, which is due to the fact that significant concentrations of released electrons are getting retrapped before they recombine with hole centres. The evaluation of kinetic parameters known as trapping parameters, i.e., E (activation energy) of the traps involved in TL emission, order of kinetics (b) and frequency factor (s) associated with the glow peaks of TL is one of the important aspects of studies in condensed matter physics. Any complete description of the material processing TL characteristics requires the knowledge of these parameters. Here, E is a measure of the energy required to eject an electron from the defect centre to the conduction band and s is the rate of electron ejection. The order of kinetics b is a measure of the probability that a free electron gets retrapped. This retrapping effect also depends on the availability of empty traps. The retrapping effect increases with the density of empty traps.

The trap parameters of deconvoluted curves are calculated using the glow curve shape method (modified by Chen). To determine the order of kinetics, the symmetry factor μ_g, which involves T_1 and T_2, is calculated (T_1 and T_2 are the temperatures corresponding to the half of the maximum intensities on either side of the glow peak maximum-T_m). Theoretically, the form factor ranges between 0.42 and 0.52. If it is close to 0.42 it says about first-order kinetics and if it is 0.52 then second order

$$\mu_g = \frac{T_m - T_2}{T_2 - T_1}. \tag{2}$$

The activation energy (E)

$$E_\alpha = c_\alpha \left(\frac{kT_m^2}{\alpha} \right) - b_\alpha (2kT_m), \tag{3}$$

where $\alpha = \tau, \delta, \omega$ with $\tau = T_m - T_1$, $\delta = T_2 - T_m$, $\omega = T_2 - T_1$,

$c_\alpha = 1.51 + 3.0(\mu_g - 0.42)$, $b_\tau = 1.58 + 4.2(\mu_g - 0.42)$,

$c_\delta = 0.976 + 7.3(\mu_g - 0.42)$, $b_\delta = 0$,

$c_\omega = 2.52 + 10.2(\mu_g - 0.42)$, $b_\omega = 1$.

The frequency factor 's' is estimated using the following expression

$$s = \frac{\beta E}{kT_m^2} \exp^{(E/kT_m)} [1 + (b-1)\Delta m]^{-1}, \tag{4}$$

where $\Delta m = 2kT_m/E$, β is the linear heating rate.

Table 1. Kinetic parameters of $ZnO : Cr^{3+}$ nanoparticles with different γ-doses.

γ-Dose	Peak	T_m (°C)	Order of kinetics	Activation energy (eV)				Frequency factor (s^{-1})
				E_τ	E_δ	E_ω	E_{avg}	
10 kGy	1	124	2	0.632	0.644	0.651	0.642	3.637E + 7
	2	215	2	0.395	0.502	0.446	0.447	3.383E + 3
	3	284	2	1.361	1.188	1.338	1.293	1.420E + 11
8 kGy	1	124	2	0.820	0.682	0.805	0.769	1.780E + 9
	2	215	2	0.670	0.372	0.602	0.548	6.350E + 4
	3	289	2	1.635	1.032	1.485	1.384	7.210E + 11
6 kGy	1	113	2	0.859	1.091	0.879	0.945	8.810E + 11
	2	156	2	0.392	0.796	0.419	0.536	3.504E + 5
	3	272	2	1.259	1.120	1.244	1.207	3.800E + 10
4 kGy	1	126	2	1.026	0.900	1.007	0.977	8.810E + 11
	2	183	2	0.403	0.665	0.446	0.505	5.534E + 4
	3	287	2	1.054	1.003	1.064	1.040	4.830E + 8
2 kGy	1	122	2	1.229	1.147	1.208	1.195	8.670E + 14
	2	172	2	0.343	0.939	0.344	0.542	2.306E + 5
	3	294	2	0.932	0.706	0.909	0.849	5.770E + 6
500 Gy	1	124	2	1.013	0.748	0.961	0.907	1.210E + 11
	2	170	2	1.183	1.604	1.201	1.329	5.780E + 14
	3	285	2	0.725	0.934	0.772	0.810	3.360E + 6

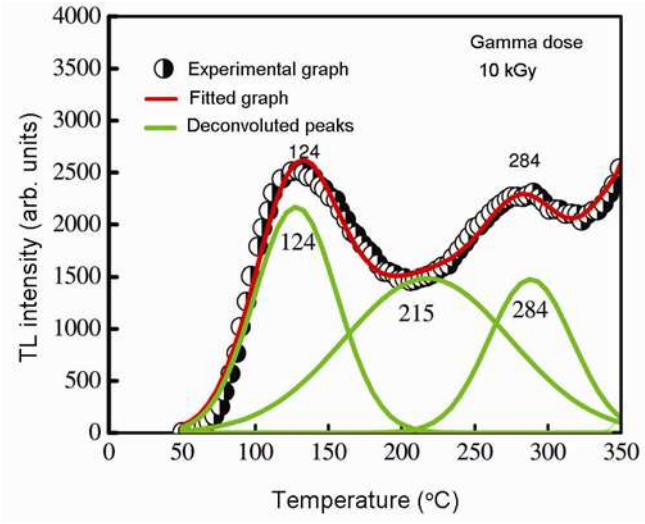

Figure 13. Deconvoluted TL glow peaks for calculation of kinetic parameters.

In the present study, the symmetry factor close to 0.52 falls under the second-order kinetics. The trapping parameters of $ZnO:Cr^{3+}$ nanoparticles irradiated with γ-rays of different doses obtained using the peak shape method (figure 13) are given in table 1.

4. Conclusions

Undoped and Cr^{3+} ZnO nanophosphors have been successfully synthesized by the solution combustion route. Particle size of $ZnO:Cr^{3+}$ is decreased as compared to undoped ZnO. Cr^{3+} doping helps in improving luminescence properties of ZnO. This can be used as red light-emitting phosphors and as TL dosimeters.

Acknowledgements

We acknowledge the DAE/BRNS project for providing financial support to carry out this research work and Chemistry TEQIP Laboratory of M.S.R.I.T. Bangalore, for providing facilities for preparation of materials.

References

1. Willander M, Nur O, Zhao Q X, Yang L, Lorenz M, Cao B, Zuniga-Perez J, Czekalla C, Zimmermann G, Grundmann M, Bakin A, Behrends A, Al-Suleiman M, El-Shaer A, Mofo A C, Postels B, Waag A, Boukos N, Travlos A, Guinard J, Dang S and Le D 2009 *Nanotechnology* **20** 332001
2. Pauporte T, Lincot D, Viana B and Pelle F 2006 *J. Appl. Phys. Lett*. **89** 233112
3. Djurisic A B, Leung Y H, Tam K H, Hsu Y F, Ding L, Ge W K, Zhong Y C, Wong K S, Chan W K, Tam H L, Cheah K W, Kwok W M and Philips D L 2007 *Nanotechnology* **18** 09570
4. Xu P S, Sun Y M, Shi C S, Xu F Q and Pan H B 2003 *Nucl. Instrum. Methods: Phys. Res. Sect. B* **19** 286
5. Elilarassi R and Chandrasekaran G 2010 *J. Optoelectron. Lett*. **6** 6
6. Chaun R, Kumar A and Choudhary R 2011 *J. Optoelectron. Biomater*. **3** 17
7. Murugadoss G 2012 *J. Mater. Sci. Technol*. **28** 487
8. Mazhdi M, Torkzadeh F and Mazhdi F M 2012 *Int. J. Bioinorg. Hybrid Nanomater*. **1** 233
9. Yuhas B D, Zitoun D O, Pauzauskie P J, He R and Yang P 2006 *Andew. Chem. Int. Ed*. **45** 420
10. Sharma P K, Datta R K and Pandey A C 2010 *J. Colloid Interface Sci.* **345** 149
11. Gurkaynak T, Altincekic and Boz I 2008 *Bull. Mater. Sci.* **31** 619
12. Pandiyarajan T and Karthikeyan B 2012 *J. Nanopart. Res*. **14** 647
13. Kumar P, Singh J, Parashar V, Singh K, Tiwari R S, Srivastava O N, Ramam K and Pandey A C 2012 *Cryst. Eng. Commun.* **14** 1653
14. Schneider L, Zaitsev S V, Jin W, Kompch A ,Winterer M and Acet Bacher M 2009 *Nanotechnology* **20** 135604
15. Pan Z, Lu Y-Y and Liu F 2012 *Nat. Mater.* **11** 58
16. Premkumar H B, Sunitha D V, Nagabhushana H, Sharma S C, Nagabhushana B M, Rao J L, Gupta K and Chakradhar R P S 2012 *J. Spectrochim. Acta Part A* **96** 154
17. Hang L, Zhioyong and Yan J 2011 *Adv. Mater. Res*. **306** 176
18. Ristić M, Musić S, Ivanda M and Popović S 2005 *J. Alloys Compd.* **397** L1
19. Tarwal N L, Jadhav P R, Vanalakar S A, Kalagi S S, Pawar R C, Shaikh J S, Mali S S, Dalavi D S, Shinde P S and Patil P S 2011 *Powder Technol.* **8** 185
20. Liu F, Yan W, Chuang Y-J, Zhen Z, Xie J and Pan Z 2013 *Sci. Rep.* **3** 1554
21. Ekambaram S, Iikubo Y and Kudo A 2006 *J. Alloys Compd*. **433** 237
22. Nagabhushana H, Nagabhushana B M, Kumar M, Premkumar H B, Shivakumara C and Chakradhar R P S 2010 *Philos. Mag.* **26** 3567
23. Mote V D, Huse V R and Dole B N 2012 *World J. Condens. Matter Phys.* **2** 208
24. Fan L, Song H, Li T, Yu L, Liu Z, Pan G, Lei Y, Bai X, Wang T, Zheng Z and Kong X 2007 *J. Lumin.* **819** 122
25. Shionoya S and Yen W H 1997 *Phosphor handbook by Phosphor Research Society* (Boca Raton, FL: CRC Press)
26. Jagannatha Reddy A, Kokila M K, Nagabhushana H, Chakradhar R P S, Shivakumara C, Rao J L and Nagabhushana B M 2011 *J. Alloys Compd.* **509** 5349
27. Gupta A, Kumar S and Bhatti H S 2010 *J. Mater. Sci.: Mater. Elect.* **21** 765
28. Jagannatha Reddy A 2012 *Structural, luminescence and EPR studies of transition metal and rare earth ion doped zinc oxide nanomaterials* PhD thesis (Bangalore University) Chapter 4, p 130
29. Lin B, Fu Z and Jia Y 2001 *Appl. Phys. Lett*. **79** 943
30. Lee J D 2012 *Concise inorganic chemistry* (Wiley India) 5th edn, p 960
31. Cruz-Vazquez C, Orante-Barron V R, Grijalva-Monteverde H, Casta V M and Bernal R 2007 *J. Mater. Lett*. **61** 1097
32. Secu C E and Sima M 2009 *Opt. Mater.* **3** 876